De novo genome assembly of *Camptotheca acuminata*, a natural source of the anti-cancer compound camptothecin

Dongyan Zhao[1], John P. Hamilton[1], Gina M. Pham[1], Emily Crisovan[1], Krystle Wiegert-Rininger[1], Brieanne Vaillancourt[1], Dean DellaPenna[2], and C. Robin Buell[1*]

[1]Department of Plant Biology, Michigan State University, East Lansing, MI 48824 USA

[2]Department of Biochemistry & Molecular Biology, Michigan State University, East Lansing, MI 48824 USA

Email addresses: Dongyan Zhao <zhaodon4@msu.edu>, John P. Hamilton <jham@msu.edu>, Gina M. Pham <phamgina@msu.edu>, Emily Crisovan <pankeyem@msu.edu>, Krystle Wiegert-Rininger <wiegertk@msu.edu>, Brieanne Vaillancourt <vaillan6@msu.edu>, Dean Dellapenna <dellapen@msu.edu>, C Robin Buell <buell@msu.edu>

*Correspondence should be addressed to: C. Robin Buell, buell@msu.edu

Manuscript type: Data note

Note: Reviewers can access the genome sequence and annotation using the following temporary URL: http://datadryad.org/review?doi=doi:10.5061/dryad.nc8qr.

Abstract

Background: *Camptotheca acuminata* is one of a limited number of species that produce camptothecin, a pentacyclic quinoline alkaloid with anti-cancer activity due to its ability to inhibit DNA topoisomerase. While transcriptome studies have been performed previously with various camptothecin-producing species, no genome sequence for a camptothecin-producing species is available to date.

Findings: We generated a high quality *de novo* genome assembly for *C. acuminata* representing 403,174,860 bp on 1,394 scaffolds with an N50 scaffold size of 1,752 kbp. Quality assessments of the assembly revealed robust representation of the genome sequence including genic regions. Using a novel genome annotation method, we annotated 31,825 genes encoding 40,332 gene models. Based on sequence identity and orthology with validated genes from *Catharanthus roseus* as well as Pfam searches, we identified candidate orthologs for genes potentially involved in camptothecin biosynthesis. Extensive gene duplication including tandem duplication was widespread in the *C. acuminata* genome with 3,315 genes belonging to 1,245 tandem duplicated gene clusters.

Conclusions: To our knowledge, this is the first genome sequence for a camptothecin-producing species, and access to the *C. acuminata* genome will permit not only discovery of genes encoding the camptothecin biosynthetic pathway but also reagents that can be used for heterologous expression of camptothecin and camptothecin analogs with novel pharmaceutical applications.

Keywords: *Camptotheca acuminata*, camptothecin, genome assembly, genome annotation, tandem duplications

Data Description

Background information on camptothecin, a key anti-cancer natural product

Camptotheca acuminata Decne, also known as the Chinese Happy Tree (Figure 1), is an eudicot asterid Cornales tropical tree species within the Nyssaceae family [1] that also contains *Nyssa* spp (tupelo) and *Davidia involucrate* (dove tree); no genome sequence is available for any member of this family. *C. acuminata* is one of a limited number of plant species that produce camptothecin, a pentacyclic quinoline alkaloid (Figure 2A) with anti-cancer activity due to its ability to inhibit DNA topoisomerase [2]. Due to poor solubility, derivatives such as irinotecan and topotecan, rather than camptothecin are currently in use as approved cancer drugs. The significance of these derivatives as therapeutics is highlighted by the listing of irinotecan on the World Health Organization Model List of Essential Medicines [3]. While transcriptome studies have been performed previously with various camptothecin-producing species including *C. acuminata* and *Ophiorrhiza pumila* (e.g., [4-6]), no genome sequence for a camptothecin-producing species is available to date. We report on the assembly and annotation of the *C. acuminata* genome, the characterization of genes implicated in camptothecin biosynthesis, and highlight the complexity of the gene complement in this species.

RNA isolation, library construction, sequencing, and transcriptome assembly

Transcriptome assemblies were constructed using nine developmental RNA-sequencing (RNA-seq) datasets described in a previous study [4] that included immature bark, cotyledons, immature flower, immature fruit, mature fruit, mature leaf, root, upper stem, and lower stem. Adapters and low-quality nucleotides were removed from the RNA-seq reads using Cutadapt (v1.8) [7] and contaminating ribosomal RNA reads were removed. Cleaned reads from all nine libraries were assembled using Trinity (v20140717) [8] with a normalization factor of 50x using default parameters. Contaminant transcripts were identified by searching the *de novo* transcriptome assembly against the National Center for Biotechnology Information (NCBI) non-redundant nucleotide database using BLAST+ (v2.2.30) [9, 10] with an E-value cutoff of 1e-5; transcripts with their best hits being a non-plant sequence were removed from the transcriptome.

For additional transcript support for use in a genome-guided transcriptome assembly to support genome annotation, strand-specific RNA-seq reads were generated by isolating RNA from root tissues and sequencing of Kappa TruSeq Stranded libraries on an Illumina HiSeq 2500 platform generating 150 nt paired-end reads (BioSample ID: SAMN06229771). Root RNA-seq reads were assessed for quality using FASTQC (v0.11.2) [11] using default parameters and cleaned as described above.

DNA isolation, library construction, and sequencing

The genome size of *C. acuminata* was estimated at 516 Mb using flow cytometry, suitable for *de novo* assembly using the Illumina platform. DNA was extracted from young leaves of *C. acuminata* at the vegetative growth stage using CTAB [12]. Multiple Illumina-compatible paired-

end libraries (Table 1) with insert sizes ranging from 180-609 bp were constructed as described previously [13] and sequenced to 150 nt in paired-end mode on an Illumina HiSeq2000. Mate-pair libraries (Table 1) with size ranges of 1.3-8.9 kb were made using the Nextera Kit (Illumina, San Diego CA) as per manufacturer's instructions and sequenced to 150 nt in paired-end mode on an Illumina HiSeq2000.

Genome assembly

Paired-end reads (Table 1) were assessed for quality using FASTQC (v0.11.2) [11] using default parameters, cleaned for adapters and low quality sequences using Cutadapt (v1.8) [7] and only reads in pairs with each read ≥25 nt were retained for genome assembly. Mate pair libraries (Table 1) were processed using NextClip (v1.3.1) [14] and only reads from Categories A, B, C were used for the assembly. Using ALLPATHS-LG (v44837) [15] with default parameters, two paired-end read libraries (180 and 268 bp insert libraries) and all five mate pair libraries (Table 1) were used to generate an initial assembly of 403.2 Mb with an N50 contig size of 108 kbp and an N50 scaffold size of 1,752 kbp (Tables 1 and 2). Gaps (5,076) in this initial assembly were filled using SOAP GapCloser (v1.12r6) [16] with four independent paired-end libraries (352, 429, 585, and 609 bp inserts, Table 1); 12,468,362 bp of the estimated 16,471,841 bp of gaps was filled leaving a total of 3,825 gaps (3,772,191 Ns). The assembly was checked for contaminant sequences based on alignments to the NCBI non-redundant nucleotide database using BLASTN (E-value = 1e-5) [10]; a single scaffold of 5,156 bp that matched a bacterium sequence with 100% coverage and 100% identity was removed. Subsequently, five scaffolds less than 1 kbp

were removed resulting in the final assembly of 403,174,860 bp comprised of 1,394 scaffolds with an N50 scaffold size of 1,752 kbp (Tables 1 and 2).

Quality assessments revealed a robust high quality assembly with 98% of the paired-end genomic sequencing reads aligning to the assembly, of which, 99.97% aligned concordantly. With respect to genic representation, 95.3% of RNA-seq-derived transcript assemblies [4] and 74,119 of 74,682 (99%) pyrosequencing transcript reads from a separate study [5] aligned to the genome assembly. A total of 93.6% of conserved Embryophyta BUSCO proteins were present in the assembly as full-length sequences with an additional 2.5% of the Embryophyta proteins fragmented [17].

Genome annotation

We used a novel genome annotation method to generate high quality annotation of the *C. acuminata* genome. We first created a *C. acuminata* specific custom repeat library (CRL) using MITE-Hunter (v2011) [18] and RepeatModeler (v1.0.8) [19]. Protein coding genes were removed from each repeat library using ProtExcluder.pl (v1.1) [20] and combined into a single CRL, which hard-masked 143.6 Mb (35.6%) of the assembly as repetitive sequence using RepeatMasker (v4.0.6) [21]. Cleaned root RNA-seq reads (Table S1, BioSample ID: SAMN06229771) were aligned to the genome assembly using TopHat2 (v2.0.13) [22] in strand-specific mode with a minimum intron length of 20 bp and a maximum intron length of 20 kb; the alignments were then used to create a genome-guided transcriptome assembly using Trinity (v2.2.0) [23]. The RNA-seq alignments were used to train AUGUSTUS (v3.1) [24] and gene predictions were generated with AUGUSTUS [25] using the hard-masked assembly. Gene

model structures were refined by incorporating evidence from the genome-guided transcriptome assembly using PASA2 (v2.0.2) [26, 27]; with the parameters: MIN_PERCENT_ALIGNED=90, MIN_AVG_PER_ID=99. After annotation comparison, models that PASA identified as being merged and a subset of candidate camptothecin biosynthetic pathways genes identified as mis-annotated were manually curated. The final high-confidence gene model set consists of 31,825 genes encoding 40,332 gene models. Functional annotation was assigned using a custom pipeline using WU-BLASTP [28] searches against the *Arabidopsis thaliana* annotation (TAIR10; [29]) and Swiss-Prot plant proteins (downloaded on 08-17-2015), and a search against Pfam (v29) using HMMER (v3.1b2) [30]. This resulted in 34,143 gene models assigned a putative function, 2,011 annotated as conserved hypothetical, and 4,178 annotated as hypothetical.

C. acuminata is insensitive to camptothecin due to mutations within its own DNA topoisomerase [31] and we identified two topoisomerase genes in our annotated gene set, one of which matches the published *C. acuminata* topoisomerase (99.78% identity, 100% coverage) and includes the two mutations that confer resistance to camptothecin (Figure 2B). Further quality assessments of our annotation with 35 nuclear-encoded *C. acuminata* genes available from GenBank revealed an average identity of 99.5% with 100% coverage in our annotated proteome while a single gene encoding 1-deoxy-D-xylulose 5-phosphate reductoisomerase (ABC86579.1) had 88.2% identity with 100% coverage that may be attributable to differences in genotypes. One mRNA reported to encode a putative strictosidine beta-D-glucosidase (AES93119.1) was found to have a retained intron that when removed, aligned with 99.3% identity yet reduced coverage (66%) as it was located at the end of a short scaffold. Collectively,

the concordant alignment of whole genome shotgun sequence reads to the assembly, the high representation of genic regions as assessed by independent transcriptome datasets (RNA-seq and pyrosequencing) as well as the core Embryophyta BUSCO proteins, when coupled with the high quality gene models as revealed through alignments with cloned *C. acuminata* genes indicate that we have not only generated a high quality genome assembly for *C. acuminata* but also a robust set of annotated gene models.

Orthology analysis

To our knowledge, *C. acuminata* is the first species within the Nyssaceae family with a genome sequence. To better understand the evolutionary relationship of *C. acuminata* with other asterids and angiosperms, we identified orthologous and paralogous groups using our annotated *C. acuminata* proteome and the proteomes of five other key species (*Arabidopsis thaliana*, *Amborella trichopoda*, *Vitis vinifera*, *Oryza sativa*, and *Catharanthus roseus*) using OrthoFinder (v0.7.1) [32] with default parameters. A total of 12,459 orthologous groups containing at least a single *C. acuminata* protein were identified with 8,521 orthologous groups common to all six species (Figure 3; Table S2). Interestingly, *C. acuminata* contains the least number of singleton genes (7,177) among the six species, and gene ontology analysis demonstrated that these genes were highly enriched in “transport”, “response to stress”, and “other cellular and biological processes” ($p < 0.0001$, χ^2 test) while dramatically under-represented in “unknown biological processes” ($p < 0.0001$, χ^2 test), suggesting these genes may be involved in stress responses and other processes specific to *C. acuminata*.

Candidate genes in the camptothecin biosynthesis pathway

While the full camptothecin biosynthetic pathway has yet to be resolved, geranylgeranyl diphosphate from the 2-*C*-methyl-D-erythritol 4-phosphate/1-deoxy-D-xylulose 5-phosphate (MEP) pathway is used to generate secologanic acid via the iridoid pathway and tryptamine from tryptophan decarboxylase are condensed by strictosidinic acid synthase to generate strictosidinic acid [33] (Figure 4A). Based on sequence identity and orthology with validated genes from *C. roseus*, we identified candidate orthologs for all steps in the MEP and iridoid pathway (Table 3). The downstream steps in camptothecin biosynthesis subsequent to formation of strictosidinic acid involve a broad set of enzymes responsible for reduction and oxidation [33] and a total of 343 cytochrome P450s (60 paralogous gene clusters and 86 singletons; Table S3) were identified which can serve as candidates for the later steps in camptothecin biosynthesis.

Though not absolute, physical clustering of genes involved in specialized metabolism has been observed in a number of species across a number of classes of specialized metabolites [34, 35]. With an N50 scaffold size of 1,752 kbp, we observed several instances of physical clustering of genes with homology to genes involved in monoterpene indole alkaloid biosynthesis which may produce related compounds in *C. acuminata*. Using validated genes involved in the biosynthesis of vinblastine and vincristine from *C. roseus* as queries [36] (Figure 4A, Table 3), we identified a single *C. acuminata* scaffold (907 kbp, 86 genes; Figure 4B) that encoded genes with sequence identity to isopentenyl diphosphate isomerase II within the MEP pathway, 8-hydroxygeraniol oxidoreductase (GOR, three complete and one partial paralogs), 7-deoxyloganic acid 7-hydroxylase (7DLH) within the iridoid pathway, and a protein with homology to *C. roseus* 16-hydroxy-2,3-dihydro-3-hydroxytabersonine N-methyltransferase (NMT) within the alkaloid

pathway suggesting that access to a high contiguity genome assembly may facilitate discovery of genes involved in specialized metabolism in *C. acuminata*.

Tandem duplicated genes and their differential expression

While fast and inexpensive, one limitation of using transcriptome assemblies solely for candidate gene discovery is the generation of chimeric transcripts if paralogs with high sequence identity are present in the transcriptome. For *C. acuminata*, it was readily apparent during our analyses of candidate camptothecin biosynthetic pathway genes that there was extensive gene duplication, including tandem duplications (e.g., Figure 4B). Paralogous clustering of the *C. acuminata* proteome revealed 5,768 paralogous groups containing 17,957 genes. We identified tandem gene duplications in the *C. acuminata* genome based on if: 1) two or more *C. acuminata* genes were present within an orthologous/paralogous group; 2) there were no more than 10 genes in between on a single scaffold; and 3) the pairwise gene distance was less than 100 kbp [37]. Under these criteria, a total of 3,315 genes belonging to 1,245 tandem duplicated gene clusters were identified as exemplified by the clustering of four GOR genes on a single scaffold (Figure 4B). Stringent alignment of genes and transcripts to a genome assembly can distinguish paralogs and their unique expression patterns attributable to neo-functionalization. Using RNA-seq datasets generated from a range of developmental tissues [4] (Tables S1 and S4), expression of paralogs from tandem duplicated gene clusters were readily distinguished as shown in Figure 5 in which nine paralogs of the late embryogenesis abundant hydroxyproline-rich glycoprotein family gene have undergone neo-functionalization at the expression level. With access to a genome assembly and a large suite of RNA-seq datasets [4]

and their corresponding metabolite data [38], we are now poised to identify and validate genes involved in the biosynthesis of camptothecin.

Uses for the *C. acuminata* genome sequence and annotation

Generation of a high-quality genome sequence and annotation dataset for *C. acuminata* will facilitate discovery of genes encoding camptothecin biosynthesis as physical clustering can be combined with co-expression data to identify candidate genes, an approach that has been extremely useful in identifying genes in specialized metabolism in a number of plant species (see [35, 36, 39]). The *C. acuminata* genome can also be used to facilitate our understanding of the mechanisms by which camptothecin production evolved independently in distinct taxa such as *C. acuminata* (Nyssaceae) and *O. pumila* (Rubiaceae). For example, a comparative analysis of *C. acuminata* and *O. pumila* may be highly informative in not only delineating genes involved in camptothecin biosynthesis but also in revealing key evolutionary events that led to biosynthesis of this critical natural product across a wide phylogenetic distance. As noted above, camptothecin is cytotoxic and as a consequence, derivatives of camptothecin are used as anti-cancer drugs. Perhaps most exciting, the ability to decipher the full camptothecin biosynthetic pathway will yield molecular reagents that can be used to not only synthesize camptothecin in heterologous systems such as yeast, but also produce less toxic analogs with novel pharmaceutical applications.

Availability of Supporting Information

Raw genomic sequence reads and transcriptome reads derived from root tissues are available in the NCBI Sequence Read Archive under project number PRJNA361128. All other RNA-seq

transcriptome reads were from Bioproject PRJNA80029 [4]. The genome assembly and annotation are available in the Dryad Digital Repository under doi (to be released upon publication), through the Medicinal Plant Genomics Resource [40] via a genome browser and search and analysis tools, and GigaDB.

Note: Reviewers can access the genome sequence and annotation using the following temporary URL: http://datadryad.org/review?doi=doi:10.5061/dryad.nc8qr.

Abbreviations

2-*C*-methyl-D-erythritol 4-phosphate/1-deoxy-D-xylulose 5-phosphate (MEP), 7-deoxyloganic acid 7-hydroxylase (7DLH), 8-hydroxygeraniol oxidoreductase (GOR), 16-hydroxy-2,3-dihydro-3-hydroxytabersonine N-methyltransferase (NMT), custom repeat library (CRL), National Center for Biotechnology Information (NCBI), RNA-sequencing (RNA-seq)

Competing Interests

The authors have declared that no competing interests exists.

Author Contributions

CRB oversaw the project. DZ performed the genome assembly, assisted in genome annotation and analyzed data. JH annotated the genome and analyzed data. EC, GP, and KWR constructed libraries and analyzed data. BV analyzed data. DDP provided intellectual oversight. DZ, JH, and CRB wrote the manuscript.

Acknowledgements

Funding for this work was provided in part by a grant to CRB and DDP from the National Institute of General Medical Sciences (1RC2GM092521) and funds to CRB and DDP from Michigan State University. The funders had no role in study design, data collection and analysis, decision to publish, or preparation of the manuscript.

Figure Legends

Figure 1. *Camptotheca acuminata* Decne, the Chinese Happy Tree, is a member in the Nyssaceae family that produces the anticancer compound camptothecin.

Figure 2. Genome aspects of *Camptotheca acuminata*. (A) Structure of camptothecin. (B) Key amino acid mutations (red rectangles) in DNA topoisomerase I in camptothecin-producing and non-producing species and their phylogenetic relationship.

Figure 3. Venn diagram showing orthologous and paralogous groups between *Camptotheca acuminata*, *Amborella trichopoda*, *Oryza sativa*, *Arabidopsis thaliana*, *Vitis vinifera*, and *Catharanthus roseus.*

Figure 4. Key portions of the proposed camptothecin biosynthetic pathway and an example of physical clustering of candidate genes in *Camptotheca acuminata*. (A) The methylerythritol phosphate (MEP) pathway (green), iridoid pathway (blue), and condensation of secologanic acid with tryptamine via strictosidinic acid synthase (STRAS) to form strictosidinic acid prior to downstream dehydration, reduction, and oxidation steps yielding camptothecin. DXS, 1-deoxy-D-xylulose 5-phosphate synthase 2; DXR, 1-deoxy-D-xylulose-5-phosphate reductoisomerase; CMS, 4-diphosphocytidyl-methylerythritol 2-phosphate synthase; CMK, 4-diphosphocytidyl-2-C-methyl-D-erythritol kinase; MCS, 2C-methyl-D-erythritol 2,4-cyclodiphosphate synthase; HDS, GCPE protein; HDR, 1-hydroxy-2-methyl-butenyl 4-diphosphate reductase; IPI, plastid isopentenyl pyrophosphate, dimethylallyl pyrophosphate isomerase; GPPS, geranyl pyrophosphate synthase; GES, plastid geraniol synthase; G8H, geraniol 8-hydroxylase; GOR, 8-hydroxygeraniol oxidoreductase; CYC1, iridoid cyclase 1; 7-DLS,

7-deoxyloganetic acid synthase; 7-DLGT, 7-deoxyloganetic acid glucosyltransferase; 7-DLH, 7-deoxyloganic acid hydroxylase; SLAS, secologanic acid synthase; TDC, tryptophan decarboxylase. **(B) Physical clustering of homologs of genes involved in the methylerythritol phosphate, iridoid, and alkaloid biosynthetic pathways of *Catharanthus roseus* on scaffold 151 of *C. acuminata*.** GOR: 8-hydroxygeraniol oxidoreductase; NMT: 16-hydroxy-2,3-dihydro-3-hydroxytabersonine N-methyltransferase; 7DLH: 7-deoxyloganic acid 7-hydroxylase; IPP2: isopentenyl diphosphate isomerase II. Gene IDs are below the arrows.

Figure 5. Expression patterns of a tandem gene cluster encoding late embryogenesis abundant hydroxyproline-rich glycoproteins across various *Camptotheca acuminata* tissues.

Table 1. Input libraries and sequences for *de novo* assembly of the *Camptotheca acuminata* genome.

BioProject ID	BioSample ID	Fragment size (bp)	No. of cleaned read pairs	Use
Paired end				
PRJNA361128	SAMN06220985	180	96,955,546	ALLPATHS-LG assembly
PRJNA361128	SAMN06220986	268	89,381,055	ALLPATHS-LG assembly
PRJNA361128	SAMN06220987	352	61,207,691	GapCloser
PRJNA361128	SAMN06220988	429	50,688,562	GapCloser
PRJNA361128	SAMN06220989	585	21,856,610	GapCloser
PRJNA361128	SAMN06220990	609	22,217,954	GapCloser
Mate pair				
PRJNA361128	SAMN06220991	8,111	9,923,643	ALLPATHS-LG assembly
PRJNA361128	SAMN06220992	7,911	7,652,519	ALLPATHS-LG assembly
PRJNA361128	SAMN06220993	1,377	12,800,554	ALLPATHS-LG assembly
PRJNA361128	SAMN06220994	3,179	13,138,503	ALLPATHS-LG assembly
PRJNA361128	SAMN06220995	8,879	13,599,241	ALLPATHS-LG assembly

All libraries were sequenced in paired end mode generating 150 nt reads.

Table 2. Metrics of the final assembly of *Camptotheca acuminata* genome.

Metric	Value
Total scaffold length (bp)	403,174,860
Total no. of scaffolds (bp)	1,394
Maximum scaffold length (bp)	8,423,530
Minimum scaffold length (bp)	1,002
N50 scaffold size (bp)	1,751,747
N50 contig size (bp)	107,594
No. Ns	3,772,191
No. gaps	3,825

Table 3. Candidate camptothecin biosynthetic pathway genes in *Camptotheca acuminata*.

Description	Abbreviation	Species	Protein	Camptotheca Gene ID	% coverage	% identity
Mevaolonate						
isopentenyl diphosphate isomerase I	IPP1	*Camptotheca acuminata*	AAB94132.1	Cac_g008847.t1	100	99.15
isopentenyl diphosphate isomerase II	IPP2	*Camptotheca acuminata*	AAB94133.1	Cac_g027591.t1	100	100.00
3-hydroxy-3-methylglutaryl coenzyme A reductase	HMGCR	*Camptotheca acuminata*	AAB69726.1	Cac_g011539.t1	100	99.48
3-hydroxy-3-methylglutaryl coenzyme A reductase	HMGCR	*Camptotheca acuminata*	AAB69727.1	Cac_g003668.t1	100	98.64
3-hydroxy-3-methylglutaryl-coenzyme A reductase	HMGCR	*Camptotheca acuminata*	AAA33040	Cac_g033987.t1	100	99.83
3-hydroxy-3-methylglutaryl-CoA synthase	HMGCS	*Camptotheca acuminata*	ACD87446.1	Cac_g028532.t1	100	95.54
MEP						
1-deoxy-D-xylulose 5-phosphate synthase 2	DXS	*Catharanthus roseus*	ABI35993.1	Cac_g024944.t1	98	77.60
1-deoxy-D-xylulose-5-phosphate reductoisomerase	DXR	*Catharanthus roseus*	AAF65154.1	Cac_g016318.t1	100	88.82
1-deoxy-D-xylulose 5-phosphate reductoisomerase	DXR	*Camptotheca acuminata*	ABC86579.1	Cac_g016318.t1	100	88.16
4-diphosphocytidyl-methylerythritol 2-phosphate synthase	CMS	*Catharanthus roseus*	ACI16377.1	Cac_g018722.t1	88	77.82
4-diphosphocytidyl-2-C-methyl-D-erythritol kinase	CMK	*Catharanthus roseus*	ABI35992.1	Cac_g021688.t1	99	76.17
2C-methyl-D-erythritol 2,4-cyclodiphosphate synthase	MCS	*Catharanthus roseus*	AAF65155.1	Cac_g008169.t1	100	73.77
GCPE protein	HDS	*Catharanthus roseus*	AAO24774.1	Cac_g022763.t1	100	88.65
1-hydroxy-2-methyl-butenyl 4-diphosphate reductase	HDR	*Catharanthus roseus*	ABI30631.1	Cac_g014659.t1	100	83.77
plastid isopentenyl pyrophosphate:dimethylallyl	IPI	*Catharanthus roseus*	ABW98669.1	Cac_g008847.t1	76	91.06

pyrophosphate isomerase						
plastid isopentenyl diphosphate isomerase	IPI	*Camptotheca acuminata*	ABI13583.1	Cac_g027591.t1	100	97.41
geranyl pyrophosphate synthase	GPPS	*Catharanthus roseus*	ACC77966.1	Cac_g026508.t1	51	76.50
10-hydroxygeraniol oxidoreductase	10HGO	*Camptotheca acuminata*	AAQ20892.1	Cac_g005530.t1	100	100.00
Iridoid						
geraniol synthase	GES	*Camptotheca acuminata*	ALL56347.1	Cac_g014037.t1	100	100.00
geraniol 8-hydroxylase	G8H	*Catharanthus roseus*	CAC80883.1	Cac_g017987.t1	95	76.71
8-hydroxygeraniol oxidoreductase	GOR	*Catharanthus roseus*	AHK60836.1	Cac_g027560.t1	100	71.69
iridoid synthase	ISY	*Catharanthus roseus*	AFW98981.1	Cac_g006027.t1	100	65.65
iridoid synthase	CYC1	*Camptotheca acuminata*	AON76722.1	Cac_g006027.t1	100	100.00
iridoid oxidase	IO	*Catharanthus roseus*	AHK60833.1	Cac_g032709.t1	97	78.44
UDP-glucose iridoid glucosyltransferase	7DLGT	*Catharanthus roseus*	BAO01109.1	Cac_g008744.t1	100	77.11
7-deoxyloganic acid 7-hydroxylase	7DLH	*Catharanthus roseus*	AGX93062.1	Cac_g012663.t1	96	69.58
loganic acid methyltransferase	LAMT	*Catharanthus roseus*	ABW38009.1	Cac_g005179.t1	95	53.91
secologanin synthase	SLS	*Catharanthus roseus*	AAA33106.1	Cac_g012666.t1	99	64.94
secologanin synthase	SLS	*Ophiorrhiza pumila*	BAP90521.1	Cac_g012666.t1	99	66.73
Alkaloid						
tryptophan decarboxylase	TDC1	*Camptotheca acuminata*	AON76721	Cac_g018974.t1	100	100.00

Note: Only the top hit from the BLAST search is presented.

References

1. Angiosperm_Phylogeny_Group_III. An update of the Angiosperm Phylogeny Group classification for the orders and families of flowering plants: APG III. Botanical Journal of the Linnean Society. 2009;161:105-21.
2. Lorence A, Nessler, C.L. Molecules of Interest: Camptothecin, over four decades of surprising findings. Phytochemistry. 2004; 65:2735–49.
3. Organization WH: 19th WHO Model List of Essential Medicines. http://www.who.int/medicines/publications/essentialmedicines/EML2015_8-May-15.pdf. Accessed 26 March 2017.
4. Gongora-Castillo E, Childs KL, Fedewa G, Hamilton JP, Liscombe DK, Magallanes-Lundback M, et al. Development of transcriptomic resources for interrogating the biosynthesis of monoterpene indole alkaloids in medicinal plant species. PLoS One. 2012;7 12:e52506. doi:10.1371/journal.pone.0052506.
5. Sun Y, Luo H, Li Y, Sun C, Song J, Niu Y, et al. Pyrosequencing of the Camptotheca acuminata transcriptome reveals putative genes involved in camptothecin biosynthesis and transport. BMC Genomics. 2011;12:533. doi:10.1186/1471-2164-12-533.
6. Yamazaki M, Mochida K, Asano T, Nakabayashi R, Chiba M, Udomson N, et al. Coupling deep transcriptome analysis with untargeted metabolic profiling in Ophiorrhiza pumila to further the understanding of the biosynthesis of the anti-cancer alkaloid camptothecin and anthraquinones. Plant Cell Physiol. 2013;54 5:686-96. doi:10.1093/pcp/pct040.
7. Martin M. Cutadapt removes adapter sequences from high-throughput sequencing reads. EMBnetjournal. 2011;17 1 doi:http://dx.doi.org/10.14806/ej.17.1.200.
8. Haas BJ, Papanicolaou A, Yassour M, Grabherr M, Blood PD, Bowden J, et al. De novo transcript sequence reconstruction from RNA-seq using the Trinity platform for reference generation and analysis. Nat Protoc. 2013;8 8:1494-512. doi:10.1038/nprot.2013.084.
9. Altschul SF, Madden TL, Schaffer AA, Zhang J, Zhang Z, Miller W, et al. Gapped BLAST and PSI-BLAST: a new generation of protein database search programs. Nucleic Acids Res. 1997;25 17:3389-402.
10. Camacho C, Coulouris G, Avagyan V, Ma N, Papadopoulos J, Bealer K, et al. BLAST+: architecture and applications. BMC Bioinformatics. 2009;10:421. doi:10.1186/1471-2105-10-421.
11. FastQC. http://www.bioinformatics.babraham.ac.uk/projects/fastqc/. Accessed 26 March 2017.
12. Saghai-Maroof MA, Soliman KM, Jorgensen RA and Allard RW. Ribosomal DNA Spacer-Length Polymorphisms in Barley - Mendelian Inheritance, Chromosomal Location, and Population-Dynamics. PRoc Natl Acad USA. 1984;81 24:8014-8. doi:Doi 10.1073/Pnas.81.24.8014.
13. Hardigan MA, Crisovan E, Hamilton JP, Kim J, Laimbeer P, Leisner CP, et al. Genome Reduction Uncovers a Large Dispensable Genome and Adaptive Role for Copy Number Variation in Asexually Propagated *Solanum tuberosum*. Plant Cell. 2016;28 2:388-405. doi:10.1105/tpc.15.00538.
14. Leggett RM, Clavijo BJ, Clissold L, Clark MD and Caccamo M. NextClip: an analysis and read preparation tool for Nextera Long Mate Pair libraries. Bioinformatics. 2014;30 4:566-8. doi:10.1093/bioinformatics/btt702.
15. Gnerre S, Maccallum I, Przybylski D, Ribeiro FJ, Burton JN, Walker BJ, et al. High-quality draft assemblies of mammalian genomes from massively parallel sequence data. Proc Natl Acad Sci U S A. 2011;108 4:1513-8. doi:1017351108.

16. Luo R, Liu B, Xie Y, Li Z, Huang W, Yuan J, et al. SOAPdenovo2: an empirically improved memory-efficient short-read de novo assembler. Gigascience. 2012;1 1:18. doi:10.1186/2047-217X-1-18.
17. Simao FA, Waterhouse RM, Ioannidis P, Kriventseva EV and Zdobnov EM. BUSCO: assessing genome assembly and annotation completeness with single-copy orthologs. Bioinformatics. 2015;31 19:3210-2. doi:10.1093/bioinformatics/btv351.
18. Han Y and Wessler SR. MITE-Hunter: a program for discovering miniature inverted-repeat transposable elements from genomic sequences. Nucleic Acids Res. 2010;38 22:e199. doi:10.1093/nar/gkq862.
19. Repeat Molder. http://www.repeatmasker.org/. Accessed 26 March 2017.
20. Campbell MS, Law M, Holt C, Stein JC, Moghe GD, Hufnagel DE, et al. MAKER-P: a tool kit for the rapid creation, management, and quality control of plant genome annotations. Plant Physiol. 2014;164 2:513-24. doi:10.1104/pp.113.230144.
21. RepeatMasker. http://www.repeatmasker.org/. Accessed 26 March 2017.
22. Kim D, Pertea G, Trapnell C, Pimentel H, Kelley R and Salzberg SL. TopHat2: accurate alignment of transcriptomes in the presence of insertions, deletions and gene fusions. Genome Biol. 2013;14 4:R36. doi:10.1186/gb-2013-14-4-r36.
23. Grabherr MG, Haas BJ, Yassour M, Levin JZ, Thompson DA, Amit I, et al. Full-length transcriptome assembly from RNA-Seq data without a reference genome. Nature Biotechnology. 2011;29 7:644-52. doi:10.1038/nbt.1883.
24. Stanke M, Schoffmann O, Morgenstern B and Waack S. Gene prediction in eukaryotes with a generalized hidden Markov model that uses hints from external sources. BMC Bioinformatics. 2006;7:62.
25. Stanke M and Morgenstern B. AUGUSTUS: a web server for gene prediction in eukaryotes that allows user-defined constraints. Nucleic Acids Res. 2005;33 Web Server issue:W465-7. doi:10.1093/nar/gki458.
26. PASA2. http://pasapipeline.github.io/. Accessed 26 March 2017.
27. Haas BJ, Delcher AL, Mount SM, Wortman JR, Smith RK, Jr., Hannick LI, et al. Improving the Arabidopsis genome annotation using maximal transcript alignment assemblies. Nucleic Acids Res. 2003;31 19:5654-66.
28. Altschul SF and Gish W. Local alignment statistics. Methods Enzymol. 1996;266:460-80.
29. The Arabidopsis Information Resource. Arabidopsis.org. Accessed 26 March 2017.
30. Eddy SR. Accelerated Profile HMM Searches. PLoS Comput Biol. 2011;7 10:e1002195. doi:10.1371/journal.pcbi.1002195.
31. Sirikantaramas S, Yamazaki M and Saito K. Mutations in topoisomerase I as a self-resistance mechanism coevolved with the production of the anticancer alkaloid camptothecin in plants. Proc Natl Acad Sci U S A. 2008;105 18:6782-6. doi:0801038105.
32. Emms DM and Kelly S. OrthoFinder: solving fundamental biases in whole genome comparisons dramatically improves orthogroup inference accuracy. Genome Biol. 2015;16:157. doi:10.1186/s13059-015-0721-2.
33. Sadre R, Magallanes-Lundback M, Pradhan S, Salim V, Mesberg A, Jones AD, et al. Metabolite Diversity in Alkaloid Biosynthesis: A Multilane (Diastereomer) Highway for Camptothecin Synthesis in Camptotheca acuminata. Plant Cell. 2016;28 8:1926-44. doi:10.1105/tpc.16.00193.
34. DellaPenna D and O'Connor SE. Plant science. Plant gene clusters and opiates. Science. 2012;336 6089:1648-9. doi:10.1126/science.1225473.
35. Nutzmann HW and Osbourn A. Gene clustering in plant specialized metabolism. Curr Opin Biotechnol. 2014;26:91-9. doi:10.1016/j.copbio.2013.10.009.

36. Kellner F, Kim J, Clavijo BJ, Hamilton JP, Childs KL, Vaillancourt B, et al. Genome-guided investigation of plant natural product biosynthesis. Plant J. 2015;82 4:680-92. doi:10.1111/tpj.12827.
37. Hanada K, Zou C, Lehti-Shiu MD, Shinozaki K and Shiu SH. Importance of lineage-specific expansion of plant tandem duplicates in the adaptive response to environmental stimuli. Plant Physiol. 2008;148 2:993-1003.
38. Wurtele ES, Chappell J, Jones AD, Celiz MD, Ransom N, Hur M, et al. Medicinal plants: a public resource for metabolomics and hypothesis development. Metabolites. 2012;2 4:1031-59. doi:10.3390/metabo2041031.
39. Itkin M, Heinig U, Tzfadia O, Bhide AJ, Shinde B, Cardenas PD, et al. Biosynthesis of antinutritional alkaloids in solanaceous crops is mediated by clustered genes. Science. 2013;341 6142:175-9. doi:10.1126/science.1240230.
40. The Medicinal Plant Genomics Resource. http://medicinalplantgenomics.msu.edu/. Accessed 26 March 2017.

Additional files

Supplemental tables:

Table S1. RNA-sequencing libraries used in this study.

BioProject ID	BioSample ID	Tissue	No. cleaned reads	Estimated bases
PRJNA80029	SAMN00255206	mature leaf	90,862,580	5,451,754,800
PRJNA80029	SAMN00255207	immature bark	84,537,958	5,072,277,480
PRJNA80029	SAMN00255208	root	88,940,668	5,336,440,080
PRJNA80029	SAMN00255215	young flower	71,435,806	4,286,148,360
PRJNA80029	SAMN00255216	immature fruit	84,250,338	5,055,020,280
PRJNA80029	SAMN00255217	mature fruit	47,811,342	2,868,680,520
PRJNA80029	SAMN00255222	cotyledons	74,037,722	4,442,263,320
PRJNA80029	SAMN00255223	upper stem	76,105,786	4,566,347,160
PRJNA80029	SAMN00255224	lower stem	72,680,940	4,360,856,400
PRJNA361128	SAMN06229771	root	55,435,804	7,224,198,331
Total			771,909,254	49,309,244,481

Table S2. Orthologous groups of genes from *Camptotheca acuminata* and five other plant species.

This is available as a separate XLS file

Table S3. P450 paralogous genes in *Camptotheca acuminata*.

This is available as a separate XLS file

Table S4. Expression abundance matrix (fragments per kbp exon model per million mapped reads) from different tissues of *Camptotheca acuminata*.

This is available as a separate XLS file

Figure 1

Click here to download Figure Figure_1.JPG

Figure 2

Click here to download Figure Fig_2.pptx

A

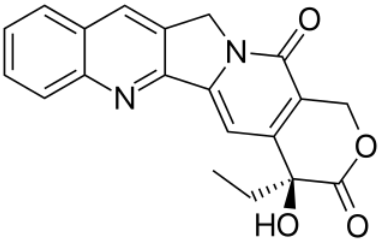

B

```
Homo sapiens AAA61207                FRGRGNHPKMGMLKRRIMPEDIIINCSKDAKVPSPPP-GHKWKEVRHDNKVTWLVSWTENIQG-S 423
Camptotheca acuminata BAG31376       FRGRGEHPKMGKLKKCIRPSDITINIGKDAPIPECPIPGESWKEIRHDNTVTWLAFWNDPIKPRE 556
Camptotheca acuminata Cac_g012488    FRGRGEHPKMGKLKKCIRPSDITINIGKDAPIPECPIPGESWKEIRHDNTVTWLAFWNDPIKPRE 555
Camptotheca acuminata Cac_g021767    FRGRGEHPKMGKLKKLIRPSDITINIGKDAPIPECPIPGESWKEIRHDNTVTWLAFWNDPINPRE 560
Ophiorrhiza pumila BAG31373          FRGRGEHPKVGKLKKRIRPRDITINIGKDAPIPECPIPGERWKEVRNDNTVTWLAYWNDPVNLKE 587
Ophiorrhiza liukiuensis BAG31374     FRGRGEHPKMGKLKKRIRPRDITINIGKDAPIPECPIPGERWKEVRNDNTVTWLAFWNDPINQKE 587
Ophiorrhiza japonica BAG31375        FRGRGEHPKMGKLKKRIRPRDITINIGKDAPIPECPIPGERWKEVRNDNTVTWLAFWIDPINQKE 588
Catharanthus roseus BAG31377         FRGRGEHPKMGKLKKRIRPCDITINIGKDAPIPECPVPGERWKEVRHDNTVTWLAFWNDPINPKE 570
Arabidopsis thaliana NP_200341       FRGRGEHPKMGKLKKRIHPCEITLNIGKGAPIPECPIAGERWKEVKHDNTVTWLAFWADPINPKE 575
Saccharomyces cerevisiae AAA35162    FXGRGAHPKTGKLKRRVNPEDIVLNLSKDAPVPPAPE-GHKWGEIRHDNTVQWLAMWRENIFN-S 355
                                     ---------------------------------------------------------
                                     Direct/indirect camptothecin binding

Homo sapiens AAA61207                ESKKKAVQRLEEQLMKLEVQATDREENKQIALGTSKINYLDPRITVAWCK 734
Camptotheca acuminata BAG31376       EALERKIGQTNAKIEKMERDKETKEGLKTIALGTSKISYLDPRITVAWCK 864
Camptotheca acuminata Cac_g012488    EALERKIGQTNAKIEKMERDKETKEGLKTIALGTSKISYLDPRITVAWCK 863
Camptotheca acuminata Cac_g021767    EALGRKIAQTSAKIEKMERDKATKEGLKTVALSTSKISYLDPRITVAWCK 868
Ophiorrhiza pumila BAG31373          EALERKIAQTNAKIEKMERDKKTKEDLKAVALSTSKISYLDPRITVAWCK 896
Ophiorrhiza liukiuensis BAG31374     ESLERKIAQTNAKIEKMERDKKTKEDLKAVALSTSKISYLDPRITVAWCK 896
Ophiorrhiza japonica BAG31375        EALERKMAQINAKIEKMERDKETKEDLKTVALGTSKINYLDPRITVAWCK 897
Catharanthus roseus BAG31377         ESLEKKIAQTNAKIEKMERDKETKEDLKTVALGTSKINYLDPRITVAWCK 880
Arabidopsis thaliana NP_200341       NAWEKKIAQQSAKIEKMERDMHTKEDLKTVALGTSKINYLDPRITVAWCK 883
Saccharomyces cerevisiae AAA35162    EKIKAQVEKLEQRIQTSSIQLKDKEENSQVSLGTSKINYIDPRLSVVFCK 738
                                     ---------------------------------------------------
                                     Direct/indirect camptothecin binding
```

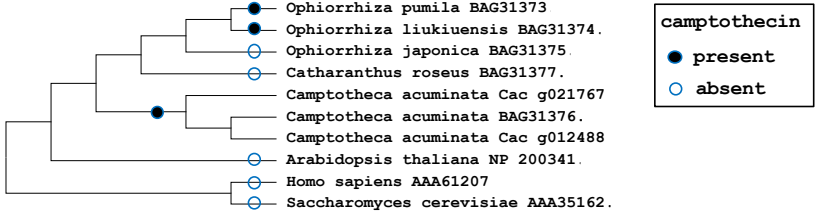

Figure 3

Click here to download Figure Fig_3.pptx

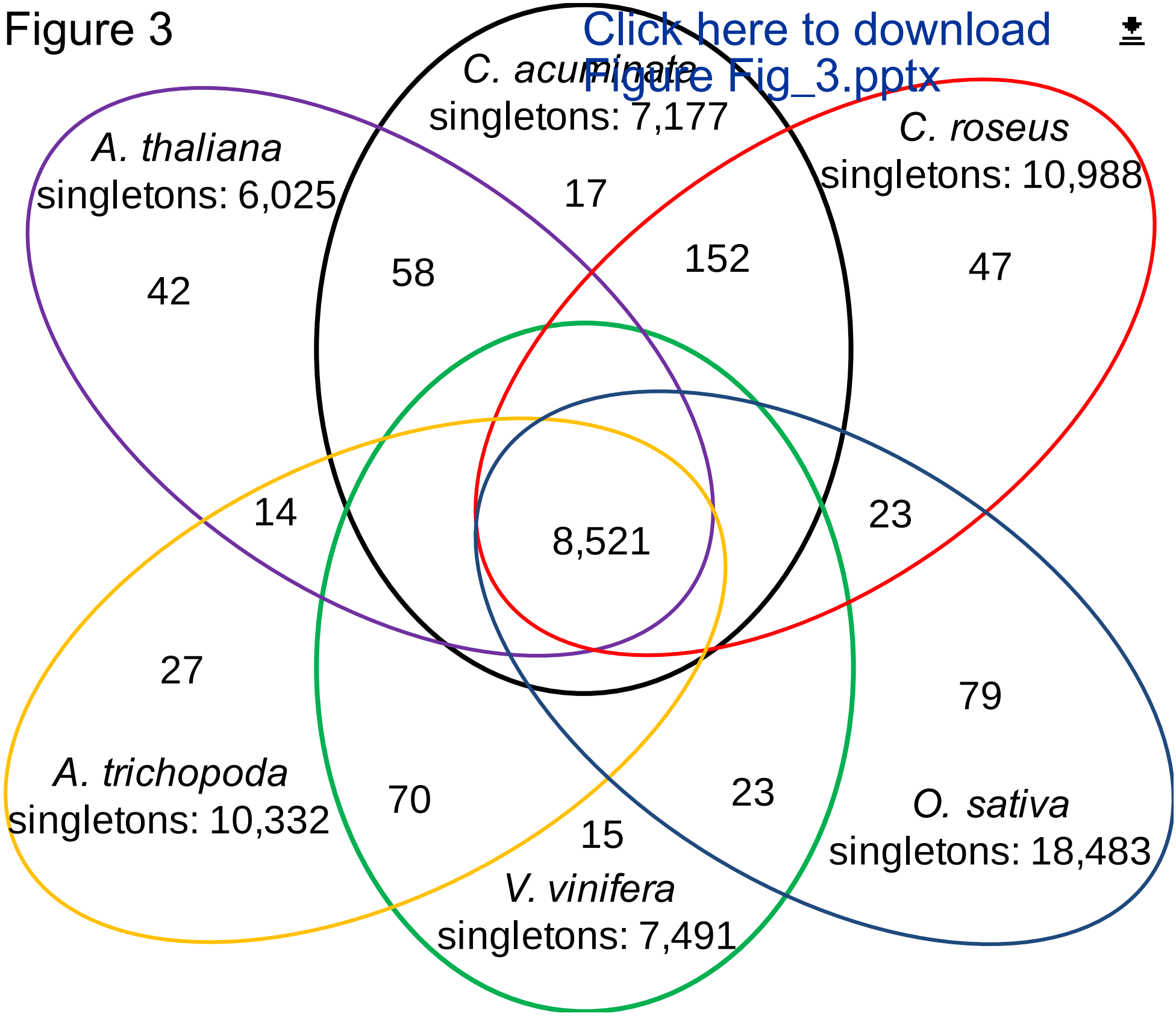

Figure 4

Click here to download Figure Fig_4.pptx

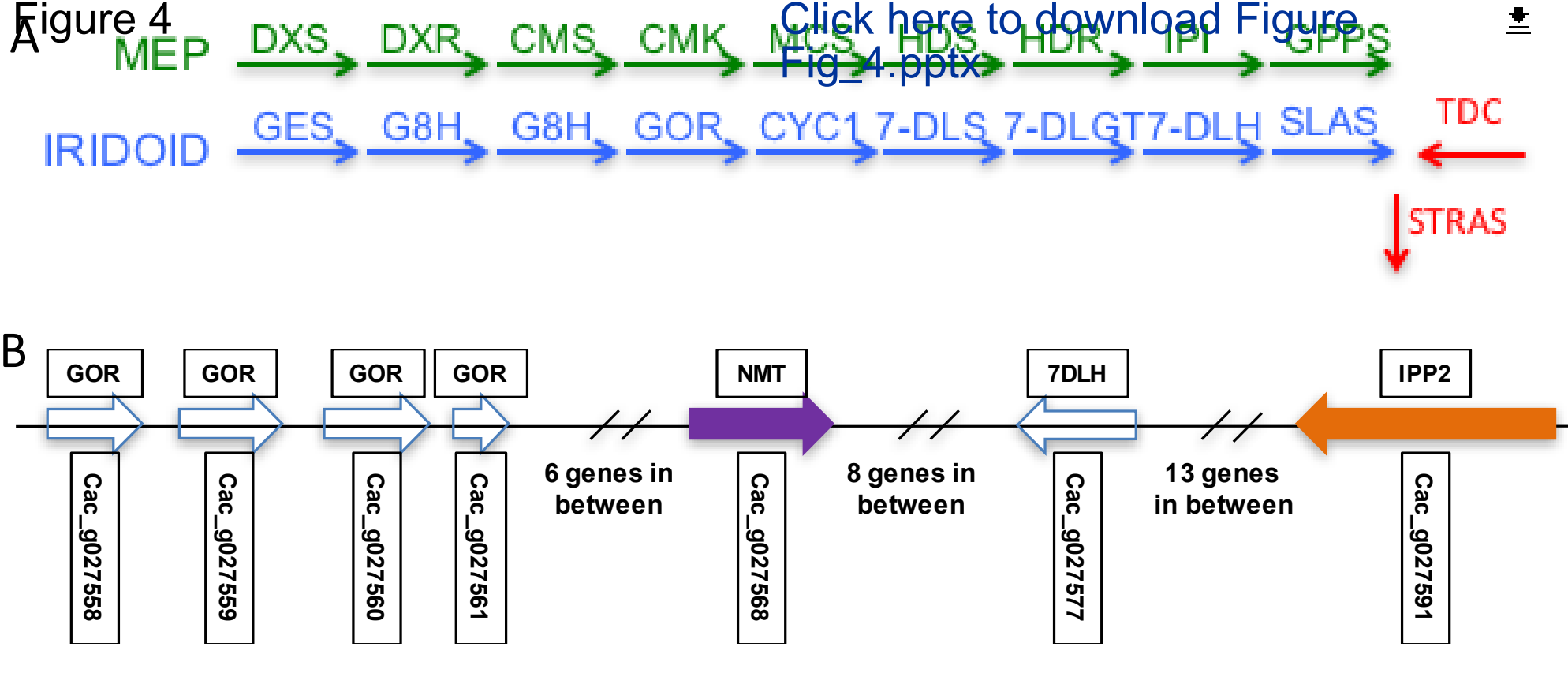

Figure 5

Click here to download Figure Fig_5.pptx

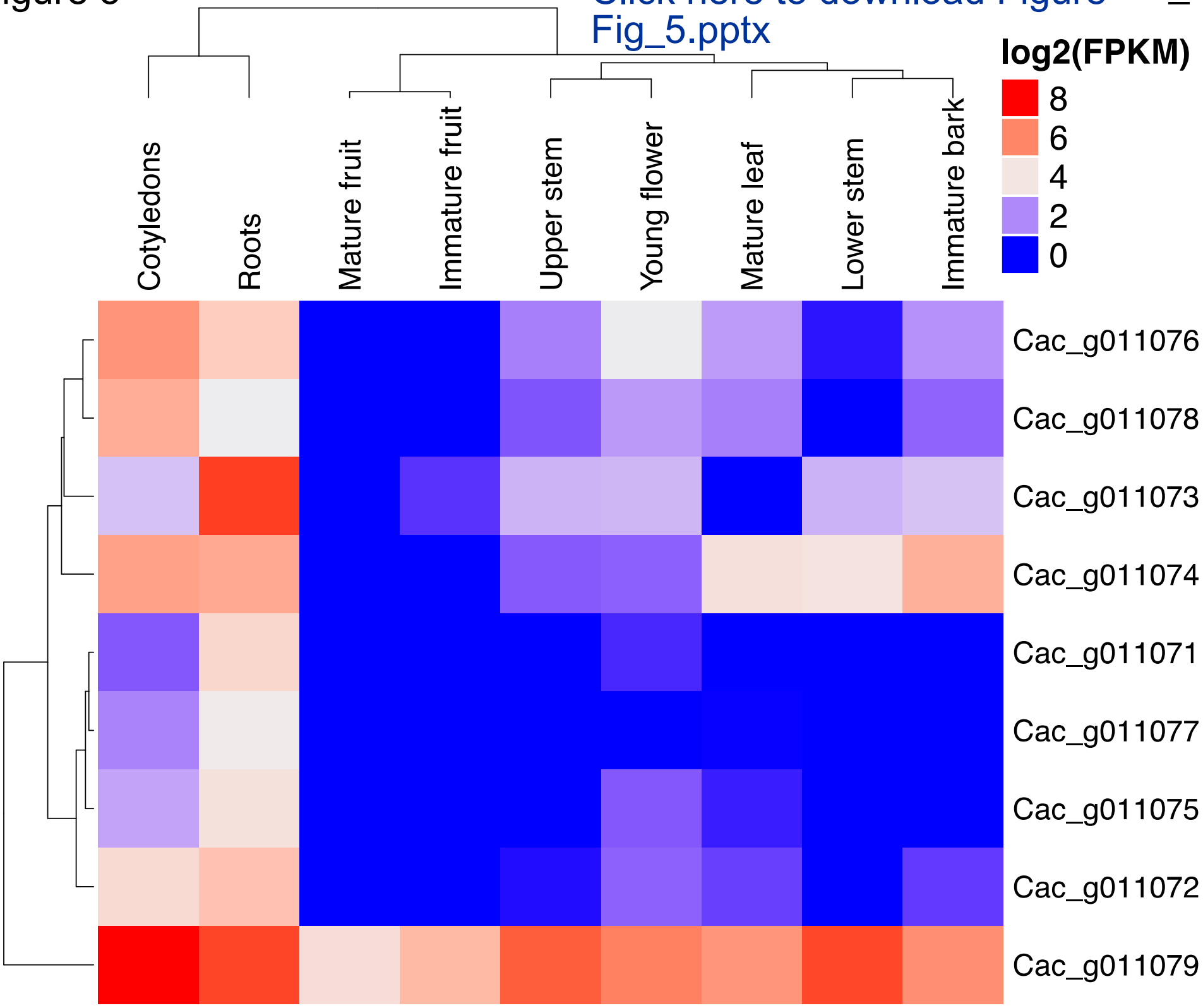

Supplementary Table 2

Supplementary Table 3

Supplementary Table 4